

Published in IET Nanobiotechnology  
 Received on 27th August 2008  
 Revised on 14th January 2009  
 doi: 10.1049/iet-nbt:20080010



# Preparation, structure and drug release behaviour of chitosan-based nanofibres

R. Zeng<sup>1,2</sup> M. Tu<sup>1,2</sup> H.-W. Liu<sup>1</sup> J.-H. Zhao<sup>1,2</sup> Z.-G. Zha<sup>2,3</sup>  
 C.-R. Zhou<sup>1,2</sup>

<sup>1</sup>Department of Materials Science and Engineering, College of Science and Engineering, Jinan University, Guangzhou 510632, People's Republic of China

<sup>2</sup>Engineering Research Center of Artificial Organs and Materials, Ministry of Education, Guangzhou 510632, People's Republic of China

<sup>3</sup>Guangzhou Overseas Chinese Hospital, the First Affiliated Hospital of Jinan University, Guangzhou 510630, People's Republic of China

E-mail: tumei@jnu.edu.cn

**Abstract:** Biomimetic polymeric nanofibres are of great interest in tissue engineering and wound repair because of their structural similarity to extracellular matrix. In this work, biomimetic chitosan-based nanofibres with various diameters were prepared by ionically cross-linking with tripolyphosphate (TPP) in adipic acid medium and characterised using transmission electron microscopy, X-ray diffraction and Fourier-transform infrared spectroscopy. Using dexamethasone sodium phosphate (DMP) and bovine serum albumin (BSA) as low and high molecular-weight bioactive molecule models, respectively, drug loading and *in vitro* release behaviours of chitosan-TPP nanofibres were investigated. The drug-loaded chitosan-TPP nanofibres showed a prolonged release profile with three distinct stages in physiological conditions because of the complicated release mechanisms involving diffusion of the drug and degradation of the nanofibre, and BSA-loaded nanofibres showed a smaller release rate than DMP-loaded nanofibres. It is proposed that biomimetic chitosan-based nanofibres may be of use in tissue engineering for sustained release of bioactive agents.

## 1 Introduction

Tissue engineering has been recognised as a promising therapeutic approach that combines cells, scaffolds and bioactive molecules such as drugs or growth factors to repair and restore damaged or diseased tissues [1, 2]. An ideal scaffold should provide the spatial and temporal microenvironment similar to that of natural tissues for regenerating cells and tissues, thus various technologies for the design and manufacture of multi-functional polymeric scaffolds mimicking the molecular regulatory characteristics and the three-dimensional architecture of the native extracellular matrix (ECM) have been developed in recent years [3–5]. For example, self-assembly, electrospinning, phase separation and so on have been used to prepare polymeric nanofibres mimicking the nano-fibrillar structure of native ECM collagen to enhance cell adhesion,

migration, proliferation and differentiated function [6, 7]. Drug delivery technology could be used in tissue engineering to provide the controlled delivery of specific bioactive factors to enhance and guide the regeneration process [8, 9].

Chitosan, a natural cationic biopolymer mainly composed of 2-amino-2-deoxy- $\beta$ -D-glucopyranose (D-glucosamine) residues, has been used extensively in biomedical and pharmaceutical applications owing to its favourable biological properties such as low toxicity, biocompatibility and biodegradability [10, 11]. In particular, chitosan complexes with various structure and properties formed by electrostatic interactions with natural or synthetic polyanions of various characteristics have attracted considerable attention, because the formation process of complexes is very simple and mild, avoiding the possible

toxicity of chemical reagents and other undesirable effects [12, 13]. For example, chitosan complex nano- or micro-particles have been widely reported as delivery systems to deliver drugs and other biologically active components, such as peptides, proteins and oligonucleotides for controlled-release oral drug delivery or localised delivery of growth factors in tissue engineering [14]. Recently, Chen *et al.* [15] successfully prepared chitosan-poly (acrylic acid) complex nanofibres using a modified dropping method in adipic acid solution to mimic the structure of ECM collagen.

In this paper, biomimetic chitosan-tripolyphosphate (TPP) nanofibres with various diameters were prepared by ionically cross-linking in adipic acid medium, and their structure and interactions were investigated. The release behaviours of dexamethasone sodium phosphate (DMP) and bovine serum albumin (BSA) from nanofibres in physiological environment were discussed and compared, as low and high molecular-weight bioactive molecule models, respectively. It was believed that chitosan nanofibres with controlled-release capacity may be a good candidate to form a biomimetic microenvironment similar to native ECM for tissue engineering.

## 2 Experimental

### 2.1 Materials

Chitosan (medium molecular weight, Brookfield viscosity: 200cps) was purchased from Aldrich, and refined twice by dissolving in dilute acetic acid solution then precipitating from dilute ammonia. Adipic acid was supplied by Sinopharm Chemical Reagent Co. Ltd. Sodium TPP was purchased from Guangzhou Chemical Reagent Factory. DMP was kindly supplied by Guangzhou Overseas Chinese Hospital, China. BSA was obtained from Sigma. All other reagents were of analytical grade and used as received.

### 2.2 Methods

**2.2.1 Preparation and characterisation of chitosan-TPP nanofibres:** Chitosan was dissolved in 2%w/v adipic acid solution at various concentrations of 0.1, 0.05 and 0.01%w/v, respectively. TPP was also dissolved in double-distilled water at 0.1, 0.05 and 0.01%w/v, respectively. The chitosan solution of different concentrations was then dropped into TPP solution of the same concentration, at a constant volume ratio of 3:1 through a syringe needle (0.45 mm in diameter), and stirring for 1 h at room temperature. The obtained chitosan-TPP nanofibres with different diameters were separated using the following procedure: the opalescent mixed solutions were ultra centrifuged, frozen at liquid N<sub>2</sub> (−196°C) and then lyophilised. To remove the remaining adipic acid, the lyophilised products were washed with 0.1 mol/L NaOH solution and double-distilled water, and then lyophilised again to obtain the final products.

The morphologies of chitosan-based nanofibres obtained under different conditions were observed by transmission electron microscopy (TEM, Philips, Tecnai-10, The Netherlands). The samples were placed on copper grids coated with carbon film, among them chitosan-based nanofibres prepared from 0.01%w/v chitosan solution were stained with 2% phosphotungstic acid for better viewing. The crystal structure of nanofibres was determined by X-ray diffraction (XRD) in a Rigaku D/max-3A diffractometer (Japan) using a Cu K $\alpha$  X-ray line at a scan rate of 8° min<sup>−1</sup> over a 2 $\theta$  range of 5 to 80°. The chemical interaction between chitosan and TPP in nanofibres was assessed by Fourier-transform infrared (FTIR) spectroscopy (Bruker, Equinox-55, Germany) in KBr.

### 2.2.2 Drug loading and *in vitro* release of chitosan-TPP nanofibres:

DMP and BSA were chosen as low and high molecular-weight bioactive molecule models, respectively, to investigate drug loading and *in vitro* drug release behaviours of chitosan-TPP nanofibres [16–18]. Briefly, DMP and BSA were dissolved into the chitosan solution of 0.1%w/v before the incorporation of TPP solution at 0.12 and 1.8 mg/mL, respectively, and then followed the above procedure to prepare the drug-loaded chitosan-based nanofibres. The obtained drug-loaded chitosan-TPP nanofibres were characterised using FTIR spectroscopy (Bruker, Equinox-55, Germany) in KBr. The amount of drug entrapped in the nanofibres was calculated based on the difference between the total amount of drug used and the amount of non-entrapped drug remaining dissolved in the aqueous suspension. Drug-loaded nanofibres were separated from the aqueous suspending medium by ultra centrifugation at 20 000 rpm for 30 min. The amount of free drug in the clear supernatant was measured by ultraviolet-visible (UV-VIS) spectroscopy at 278 nm for DMP, while 280 nm for BSA, using a Jasco V-550 spectrophotometer (Japan). And the supernatant of non-loaded nanofibres was measured as basic correction. Each experiment was performed in triplicate. The drug loading capacity (LC) of nanofibres and the drug loading efficiency (LE) of the process were calculated from (1) and (2) indicated below

$$LC = (A - B)/C \times 100\% \quad (1)$$

$$LE = (A - B)/A \times 100\% \quad (2)$$

where  $A$  is the total amount of drug,  $B$  is the amount of free drug in supernatant and  $C$  is the weight of nanofibres.

The drug release behaviours of drug-loaded chitosan-TPP nanofibres were studied in physiological conditions. 50 mg DMP- or BSA-loaded nanofibres were suspended in 50 ml PBS solution ( $pH$  7.4) incubated on a shaking water-bath at  $37.0 \pm 0.5^\circ\text{C}$ , 50 rpm, and sampled at predetermined intervals and adding an equal volume of fresh buffer solution to maintain a constant volume of releasing medium. After ultra centrifugation at 20 000 rpm for

30 min, the amount of released drug from the nanofibres collected at each time intervals was determined by UV-VIS spectrophotometric measurements at 278 nm for DMP, whereas 280 nm for BSA. Each experiment was repeated in triplicate.

### 3 Results and discussion

#### 3.1 Morphology and structure of chitosan-based nanofibres

It is well known that the formation of chitosan complexes in aqueous solutions depends on not only the degree of deacetylation and molecular weight of chitosan, the chemical structure of polyanions, but also their reaction conditions such as  $pH$ , acidic medium, ionic strength, concentration, mixed ratio and duration and temperature of the interaction. By controlling the above factors, chitosan complexes with various structure and properties could be obtained. Fig. 1 shows TEM images of chitosan-TPP nanofibres formed by ionically cross-linking at various chitosan concentrations in adipic acid medium. It could be seen that chitosan-TPP nanofibres with various diameters and the length up to several microns were prepared under the conditions used, and the diameter of obtained nanofibres was affected by chitosan concentration. For the chitosan concentration of 0.1, 0.05 and 0.01%w/v, the average diameter of nanofibres was about 200, 180 and

40 nm, respectively. The decrease of the concentration of chitosan induced the decrease of the average diameter of nanofibres, which provided an approach for controlling the average diameter of chitosan-TPP nanofibres by changing the concentration of chitosan. Since the most abundant ECM protein, collagen, possesses a fibrous structure with fibre bundle diameter varying from 50 to 500 nm [5], the obtained chitosan-TPP nanofibres had the similar scale to those of natural ECM, and could be used as a biomimetic scaffold material in tissue engineering.

The formation of chitosan-TPP nanofibrous structure was related to the chemical steric structure and the hydrocarbon chain length of carboxylic acid used, adipic acid. In fact, the formation of chitosan-TPP complexes in aqueous solutions was mainly caused by ionic interaction between the cationic chitosan and anionic TPP leading to interpolymer linkages, and the so-called ionic gelation process. However, the morphologies of complexes formed in aqueous solutions were also affected by the characteristics of carboxylic acid used, as the configuration of chitosan and its interaction with TPP were greatly influenced by the two types of interactions between chitosan and carboxylic acid: the ionic interaction between the functional groups of carboxylic acid, the amine group of chitosan and the hydrophobic interaction between internal domains of chitosan helices, and hydrocarbon chains of carboxylic acid [19]. Adipic acid with the large chain

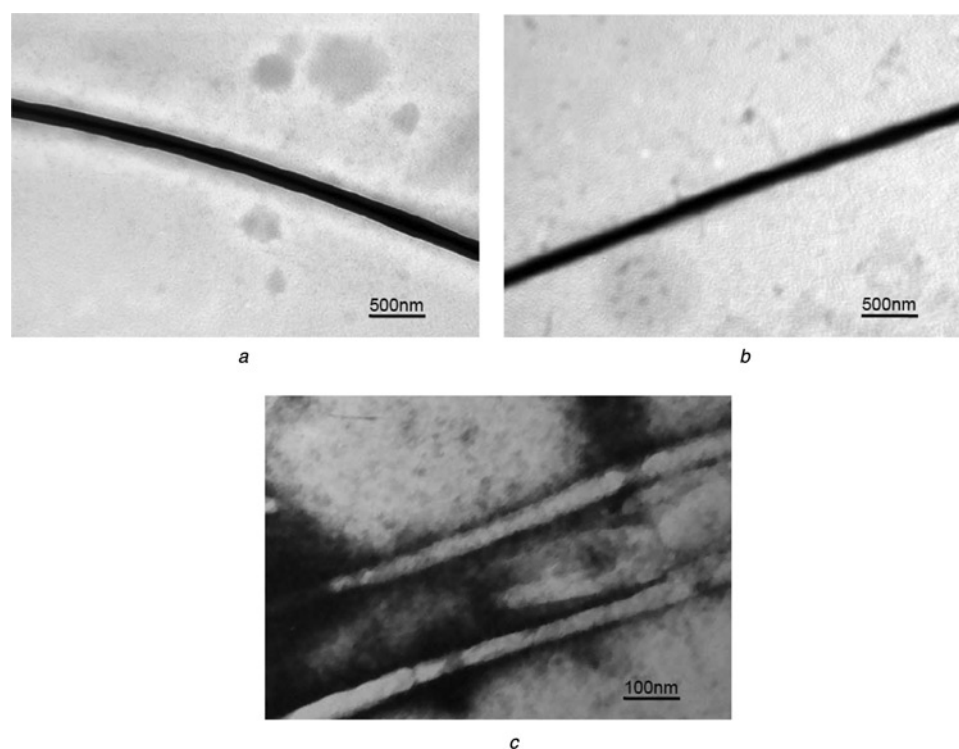


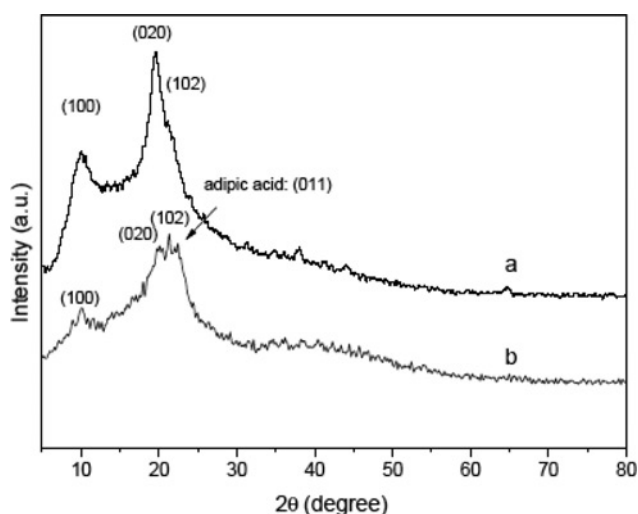
**Figure 1** TEM images of chitosan-TPP nanofibres formed by ionically cross-linking in adipic acid medium at different chitosan concentration of

- a 0.1%w/v
- b 0.05%w/v
- c 0.01%w/v

length and two carboxylic groups might act as a template to induce chitosan-TPP complex to form a nanofibrous structure in aqueous solution.

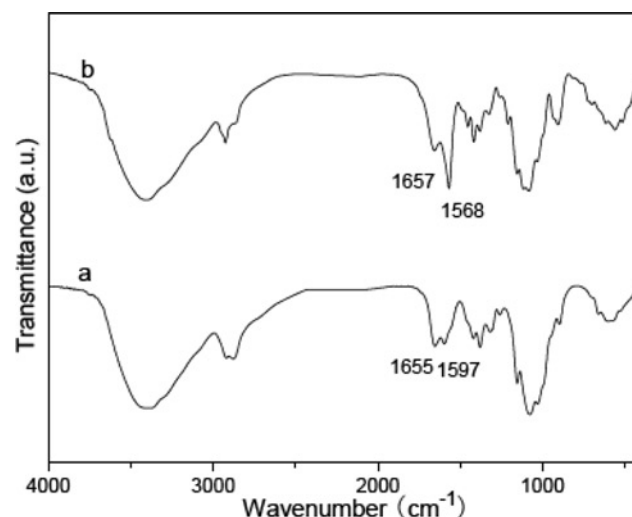
Fig. 2 demonstrates the XRD patterns of refined chitosan and chitosan-TPP nanofibres obtained from 0.1%w/v chitosan solution. The XRD pattern of chitosan-TPP nanofibres obtained in adipic acid medium showed a broad triplicate peak at  $2\theta$  of around  $21^\circ$ , whereas the frozen-dried refined chitosan showed a broad peak at  $20.0^\circ$  with a shoulder at  $21.8^\circ$  assigned to (0 2 0) and (1 0 2) reflection, respectively. The new peak could be ascribed to the (0 1 1) reflection from adipic acid [20]. The results suggested that there was some residue of adipic acid in chitosan-TPP nanofibres that would influence the crystal structure of nanofibres.

Fig. 3 shows the FTIR spectra of chitosan and chitosan-TPP nanofibres obtained from 0.1%w/v chitosan solution in adipic acid medium. For the pure chitosan, the carbonyl stretching (amide I band) at  $1655\text{ cm}^{-1}$  and  $\text{NH}_2$  bending (amide II band) at  $1597\text{ cm}^{-1}$  could be clearly observed. The broad band ascribed to the stretching vibration of  $-\text{NH}_2$  and  $-\text{OH}$  group appeared at  $3400\text{--}3500\text{ cm}^{-1}$ , and the absorption bands at  $1000\text{--}1200\text{ cm}^{-1}$  were attributed to its saccharine structure [21]. Compared with that of chitosan, the absorption band assigned to the stretching vibration of  $-\text{CH}_2-$  at  $2920\text{ cm}^{-1}$  increased, and the amide II band shifted to  $1568\text{ cm}^{-1}$  for chitosan-TPP nanofibres, although the amide I band had almost no shift. And the relative intensity of amide II band to amide I band also increased greatly for chitosan-TPP nanofibres. The results indicated that some interaction have occurred between  $-\text{NH}_2$  groups of chitosan and TPP in the nanofibres.



**Figure 2** XRD patterns of chitosan and chitosan-TPP nanofibres obtained from 0.1%w/v chitosan solution

a Chitosan  
b Chitosan-TPP



**Figure 3** FTIR spectra of chitosan and chitosan-TPP nanofibres obtained from 0.1%w/v chitosan solution

a Chitosan  
b Chitosan-TPP

### 3.2 Model drug loading and in vitro release of chitosan-TPP nanofibres

Chitosan-TPP nano- or micro-complexes have been successfully used to load drugs and other biologically active molecules, such as peptides, proteins and oligonucleotides for controlled release. And their drug LC and drug LE were significantly affected by the physico-chemical characteristics and initial concentration of drug. On the basis of the measurement of UV-VIS, the drug LC and drug LE of chitosan-TPP nanofibres under the conditions used were  $12.0 \pm 1.2$  and  $90.0 \pm 1.7\%$  for DMP, whereas it was  $50.3 \pm 2.4$  and  $56.3 \pm 3.0\%$  for BSA, respectively. The large size of BSA with 68 kDa would hinder the encapsulation of BSA into the nanofibres and lead to a lower LE value.

FTIR spectra of chitosan-TPP nanofibres and drug-loaded chitosan-TPP nanofibres are shown in Fig. 4. It could be seen that the broad band ascribed to the stretching vibration of  $-\text{NH}_2$  and  $-\text{OH}$  group at  $3400\text{--}3500\text{ cm}^{-1}$ , and the absorption band assigned to the stretching vibration of  $-\text{CH}_2-$  at  $2920\text{ cm}^{-1}$  almost disappeared in the case of DMP- and BSA-loaded nanofibres, compared with that of chitosan-TPP nanofibres. In addition, the amide I and amide II band for DMP-loaded nanofibres shifted to  $1635$  and  $1535\text{ cm}^{-1}$ , respectively, while whereas the amide I and amide II band for BSA-loaded nanofibres shifted to  $1639$  and  $1535\text{ cm}^{-1}$ , respectively. And the relative intensity of the amide II band to amide I band also decreased greatly after drug loading. The results indicated that the incorporation of both DMP and BSA would affect the interaction between  $-\text{NH}_3^+$  of chitosan and TPP. For example, the acid group of BSA may compete with TPP in their

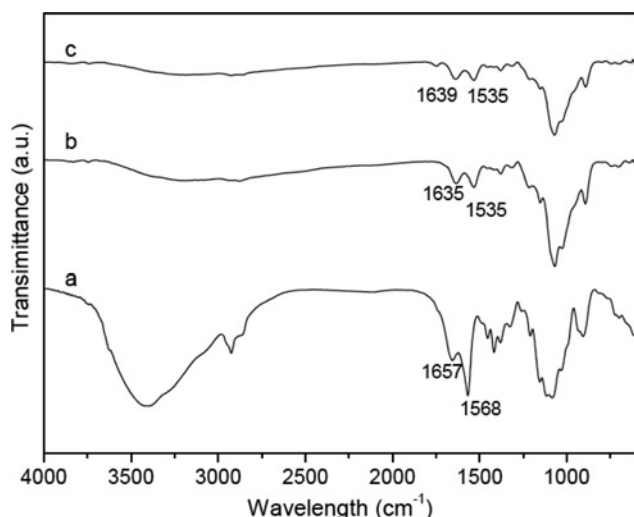


**Figure 4** FTIR spectra of chitosan-TPP nanofibres, DMP-loaded chitosan-TPP nanofibres and BSA-loaded chitosan-TPP nanofibres obtained from 0.1%w/v chitosan solution

- a Chitosan-TPP nanofibres  
b DMP-loaded chitosan-TPP nanofibres  
c BSA-loaded chitosan-TPP nanofibres

interaction with  $-\text{NH}_3^+$  of chitosan, thus limit the interaction between chitosan and TPP.

The model drug *in vitro* release behaviours from drug-loaded chitosan-TPP nanofibres in physiological conditions are shown in Fig. 5. As can be seen, both DMP-loaded and BSA-loaded nanofibres exhibited a releasing profile with three stages under the conditions used. Since the release of a bioactive agent from a biodegradable polymeric delivery system is primarily controlled by diffusion of the bioactive agent through the polymer and degradation of the polymer, the release profile with three distinct phases is

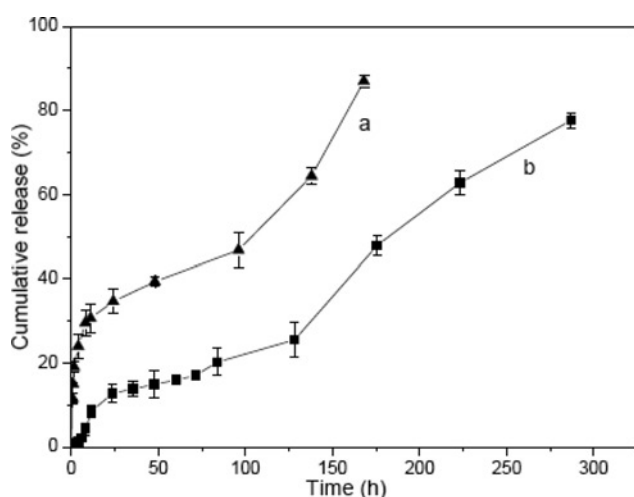


**Figure 5** Release of DMP and BSA from drug-loaded chitosan-TPP nanofibres obtained from 0.1%w/v chitosan solution in PBS at  $37.0 \pm 0.5^\circ\text{C}$

- a DMP  
b BSA

usually observed for biodegradable polymers that includes the initial period of burst release, which is related to the rapid diffusion of the active agent located close to the surface of the polymer; the second period of minimal release, during which the polymer is gradually degraded but has not yet decreased sufficiently in molecular weight to lead an increased release rate; and the third period with the increased release rate, which results from the massive degradation of the polymer [22]. Moreover, the release behaviours of a biodegradable polymeric delivery system were influenced by the molecular size of the bioactive agent and loading percentage into the polymer, as well as polymer composition, molecular weight, the dimensions and shape of the matrix [23].

In the case of DMP-loaded nanofibres, the release profile exhibited a burst release of 30% in the first 12 h, which associated with diffusion of DMP dispersing close to the nanofibres surface, and then a slow release till about 100 h mainly because of the gradual degradation of nanofibres, and then a faster release resulted from the massive degradation of nanofibres. Totally  $\sim 87.0\%$  of DMP was released from the DMP-loaded chitosan-TPP nanofibres within 160 h. As for BSA-loaded nanofibres, the release profile showed an initial burst release of 8.5% in the first 12 h, and then a second minimal release stage till about 150 h and the third period with the increased release rate of BSA. Totally about 77.6% of BSA was released from the BSA-loaded chitosan-TPP nanofibres within 280 h. Compared with DMP-loaded chitosan-TPP nanofibres, BSA-loaded chitosan-TPP nanofibres showed a smaller release rate of BSA because of the larger molecular weight of BSA. The results also suggested that chitosan-TPP nanofibres may provide a prolonged release of bioactive agents in physiological conditions.

## 4 Conclusion

Biomimetic chitosan-TPP nanofibres with various diameters were successfully prepared by ionically cross-linking with the aid of adipic acid under mild conditions, and the average diameter of the nanofibres could be controlled by changing the concentration of chitosan. It was found that some interaction has occurred between the amine groups of chitosan and TPP in the nanofibres, and the loaded bioactive molecules would affect this interaction. The bioactive molecules release from chitosan-TPP nanofibres in physiological conditions showed a prolonged release profile with three distinct stages including the initial burst release, the slow release stage, and then fast release stage, which resulted from the combination of two release mechanisms: the diffusion of bioactive molecules and the degradation of nanofibres. And the release behaviours of bioactive molecules were dependent on their molecular size, the release of BSA from chitosan-TPP nanofibres was slower than that of DMP. The results suggested that biomimetic chitosan-TPP nanofibres were able to provide a prolonged release of bioactive agents in physiological

conditions, which may be used in tissue engineering to provide a biomimetic microenvironment similar to the natural ECM for regenerative cells and tissues.

## 5 Acknowledgments

The authors would like to acknowledge financial support from the National Natural Science Foundation of China (No. 20504018) and the National High Technology Research and Development Program of China (863 Program) (No. 2007AA09Z440).

## 6 References

- [1] LANGER R., VACANTI J.P.: 'Tissue engineering', *Science*, 1993, **260**, (5110), pp. 920–926
- [2] LAVIK E., LANGER R.: 'Tissue engineering: current state and perspectives', *Appl. Microbiol. Biotechnol.*, 2004, **65**, (1), pp. 1–8
- [3] INGBER D.E., MOW V.C., BUTLER D. ET AL.: 'Tissue engineering and developmental biology: going biomimetic', *Tissue Eng.*, 2006, **12**, (12), pp. 3265–3283
- [4] CHUNG H.J., PARK T.G.: 'Surface engineered and drug releasing pre-fabricated scaffolds for tissue engineering', *Adv. Drug Deliv. Rev.*, 2007, **59**, (4–5), pp. 249–262
- [5] MA P.X.: 'Biomimetic materials for tissue engineering', *Adv. Drug Deliv. Rev.*, 2008, **60**, (2), pp. 184–198
- [6] BARNES C.P., SELL S.A., BOLAND E.D., SIMPSON D.G., BOWLIN G.L.: 'Nanofiber technology: designing the next generation of tissue engineering scaffolds', *Adv. Drug Deliv. Rev.*, 2007, **59**, (14), pp. 1413–1433
- [7] TOH Y.-C., NG S., KHONG Y.M. ET AL.: 'Cellular responses to a nanofibrous environment', *Nanotoday*, 2006, **1**, (3), pp. 34–43
- [8] SOKOLSKY-PAPKOV M., AGASHI K., OLAYE A., SHAKESHEFF K., DOMB A.J.: 'Polymer carriers for drug delivery in tissue engineering', *Adv. Drug Deliv. Rev.*, 2007, **59**, (4–5), pp. 187–206
- [9] BIONDI M., UNGARO F., QUAGLIA F., NETTI P.A.: 'Controlled drug delivery in tissue engineering', *Adv. Drug Deliv. Rev.*, 2008, **60**, (2), pp. 229–242
- [10] RAVI KUMAR M.N.V., MUZZARELLI R.A.A., MUZZARELLI C., SASHIWA H., DOMB A.J.: 'Chitosan chemistry and pharmaceutical perspectives', *Chem. Rev.*, 2004, **104**, (12), pp. 6017–6084
- [11] YI H., WU L.-Q., BENTLEY W.E. ET AL.: 'Biofabrication with chitosan', *Biomacromolecules*, 2005, **6**, (6), pp. 2881–2894
- [12] BERGER J., REIST M., MAYER J.M., FELT O., PEPPAS N.A., GURNY R.: 'Structure and interactions in covalently and ionically crosslinked chitosan hydrogels for biomedical applications', *Eur. J. Pharm. Biopharm.*, 2004, **57**, (1), pp. 19–34
- [13] IL'INA A.V., VARLAMOV V.P.: 'Chitosan-based polyelectrolyte complexes: a review', *Appl. Biochem. Micro.*, 2005, **41**, (1), pp. 5–11
- [14] AGNIHOTRI S.A., MALLIKARJUNA N.N., AMINABHAVI T.M.: 'Recent advances on chitosan-based micro- and nanoparticles in drug delivery', *J. Control. Release*, 2004, **100**, (1), pp. 5–28
- [15] CHEN C.-Y., WANG J.-W., HON M.-H.: 'Polyion complex nanofibrous structure formed by self-assembly of chitosan and poly(acrylic acid)', *Macromol. Mater. Eng.*, 2006, **291**, (2), pp. 123–127
- [16] SHU X.Z., ZHU K.J.: 'Controlled drug release properties of ionically cross-linked chitosan beads: the influence of anion structure', *Int. J. Pharm.*, 2002, **233**, (1–2), pp. 217–225
- [17] POLK A., AMSDEN B., YAO K.D., PENG T., GOOSEN M.F.A.: 'Controlled release of albumin from chitosan-alginate microcapsules', *J. Pharm. Sci.*, 1994, **83**, (2), pp. 178–185
- [18] XU Y., DU Y.: 'Effect of molecular structure of chitosan on protein delivery properties of chitosan nanoparticles', *Int. J. Pharm.*, 2003, **250**, (1), pp. 215–226
- [19] SHAMOV M.V., BRATSKAYA S.Y., AVRAMENKO V.A.: 'Interaction of carboxylic acids with chitosan: effect of pK and hydrocarbon chain length', *J. Colloid Interface Sci.*, 2002, **249**, (2), pp. 316–321
- [20] KARADEDELI B., BOZKURT A., BAYKAL A.: 'Proton conduction in adipic acid/benzimidazole hybrid electrolytes', *Physica B*, 2005, **364**, (1–4), pp. 279–284
- [21] AROF A.K., OSMAN Z.: 'FTIR studies of chitosan acetate based polymer electrolytes', *Electrochim. Acta*, 2003, **48**, (8), pp. 993–999
- [22] SILVA G.A., DUCHEYNE P., REIS R.L.: 'Materials in particulate form for tissue engineering. 1. Basic concepts', *J. Tissue. Eng. Regen. Med.*, 2007, **1**, (1), pp. 4–24
- [23] LANGER R.: 'Drug delivery dystems', *MRS Bull*, 1991, **XVI**, pp. 47–49